Supplementary Information to:

Albumin-driven disassembly of lipidic nanoparticles: the specific case of the squalene-adenosine nanodrug

Frédéric Gobeaux[1,*], Joëlle Bizeau[1], Firmin Samson[1], Laurent Marichal[1,2], Isabelle Grillo[3], Frank Wien[4], Semen O. Yesylevsky[5], Christophe Ramseyer[6], Marie Rouquette[7], Sinda Lepêtre-Mouelhi[7], Didier Desmaële[7], Patrick Couvreur[7], Patrick Guenoun[1], Jean-Philippe Renault[1], Fabienne Testard[1,*]

[1] LIONS - NIMBE CEA, CNRS, Université Paris-Saclay, CEA Saclay, 91191 Gif-sur-Yvette Cedex, France

[2] I2BC, JOLIOT, DRF, CEA, CNRS, Université Paris-Saclay, Gif-sur-Yvette, France

[3] Institut Laue Langevin, 71 avenue des martyrs, B.P. 156, 38042 Grenoble Cedex 9, France

[4] SOLEIL Synchrotron, Saint Aubin, France

[5] Department of Physics of Biological Systems, Institute of Physics of the National Academy of Sciences of Ukraine, Prospect Nauky 46, 03028 Kyiv, Ukraine

[6] Laboratoire Chrono Environnement UMR CNRS 6249, Université de Bourgogne Franche-Comté, 16 route de Gray, 25030 Besançon Cedex, France.

[7] Institut Galien Paris-Sud, UMR 8612, CNRS, Université Paris-Sud, Université Paris-Saclay, Faculté de Pharmacie, 5 rue Jean-Baptiste Clément, F-92296 Châtenay-Malabry Cedex, France.

Correspondance: * **frederic.gobeaux@cea.fr**, * **fabienne.testard@cea.fr**

1. ^{1}H NMR

Squalenylacetic-acid adenosine or *(4E,8E,12E,16E,20E)-N-{9-[(2R,5R)*-3,4-dihydroxy-5-(hydroxymethyl)oxolan-2-yl]-9*H*-purin-6-yl}-4,8,12,17,21,25- hexamethylhexacosa-4,8,12,16,20,24-hexaenamide (SQAd)

^{1}H NMR (300 MHz, $CDCl_3$) δ: 9.37 (broad s, 1 H, N*H*CO), 8.51 (s, 1 H, H8), 8.21 (s, 1 H, H2), 5.97 (d, 1 H, *J* = 6.1 Hz, H1'), 5.22-4.99 (m, 6 H, *H*C=C(CH_3)), 4.93 (m, 1 H, *J* = 4.9 Hz, H2'), 4.47 (m, 1 H, H3'), 4.32 (m, 1 H, H4'), 3.91 (d, 1 H, *J* = 11.85 Hz, H5'), 3.79 (d, *J* = 11.85 Hz, H5'), 3.19 (t, CH_2(α), 8H, $[N(nBu)_4]^+$ residual salt), 2.88 (m, 2 H, CH_2-C*H*$_2$-CO_2), 2.41 (m, 2 H, C*H*$_2$-CH_2-CO_2), 2.21-1.84 (m, 20 H, =C(CH_3)C*H*$_2$C*H*$_2$), 1.80-1.59 ((m, 21 H, C=C(C*H*$_3$)) + (16H, CH_2(β), CH_2(γ), $[N(nBu)_4]^+$ residual salt)), 1.59-1.11 (m, impurities), 0.98 (t, *J* = 7.25 Hz, CH_3(δ), 12H, $[N(nBu)_4]^+$) 0.96-0.73 (m, impurities)

2. Additional SANS characterization and analysis

Reproducibility of the nanoprecipitation process

Different samples of SQAd nanoparticles have been prepared with similar nanoprecipitation protocol. The Figure S1 shows the different SANS patterns obtained for 4 different solutions prepared in D_2O with the same synthetic batch of SQAd bioconjugate. All the curves are nearly superimposed in the small and medium *q* range, demonstrating the repeatability in sample preparation for the size distribution of the colloidal dispersion. In the large *q* range, the differences come from the residual ethanol in the sample.[1]

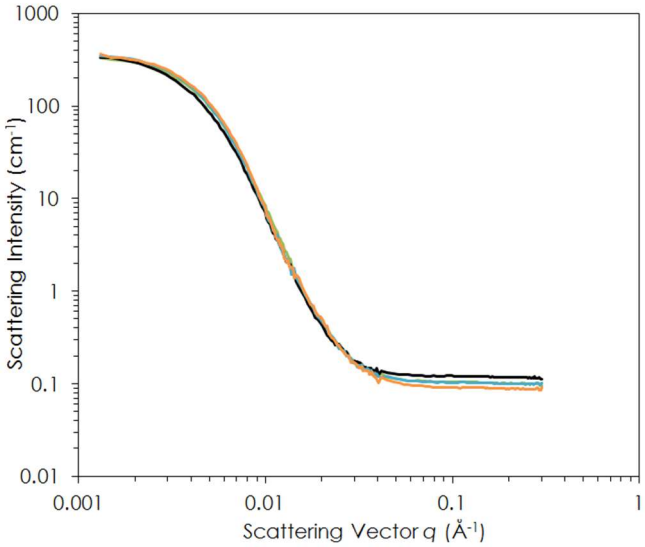

Figure S1: SANS patterns of 4 different samples of independently nanoprecipitated SQAd nanoparticles.

Stability of the nanoparticles upon dilution in water

The SQAd nanoparticles are stable by dilution in water. The SANS patterns of the different solutions whose intensity has been normalized by the dilution factor are indeed superimposed (Figure S2B).

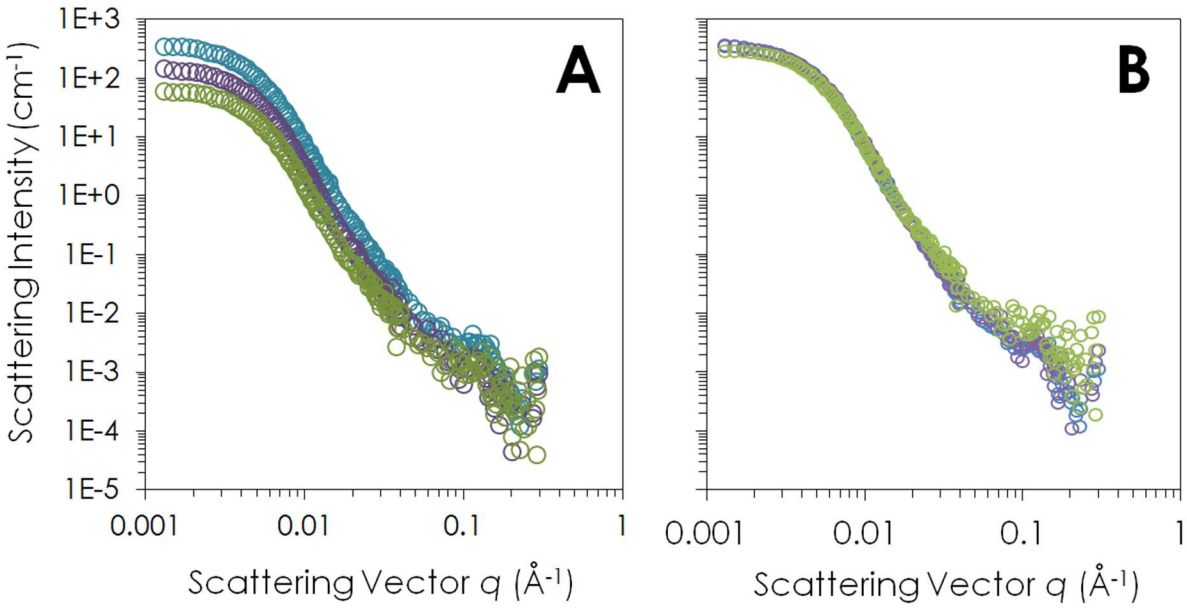

Figure S2: A) SANS patterns of SQAd/D_2O at 3 different concentrations (1, 0.4 and 0.2 mg/ml). **B)** Same SANS patterns with intensity normalized by the dilution factor (i.e. 1, 2.5 and 5).

SANS characterization of BSA solution

The SANS patterns obtained for BSA in PBS can be fitted by ellipsoids (Figure S3), in agreement with the literature.[2–4] This fit was used as a reference curve in the linear combination used to fit the SANS curves of the BSA/SQAd mixtures (it was thus recalculated for the proper *q*-range). The estimated BSA concentration in FBS (Figure 2B) comes from the comparison of the scattered intensity of a 13 mg/ml BSA solution, which is 3.1 times lower.

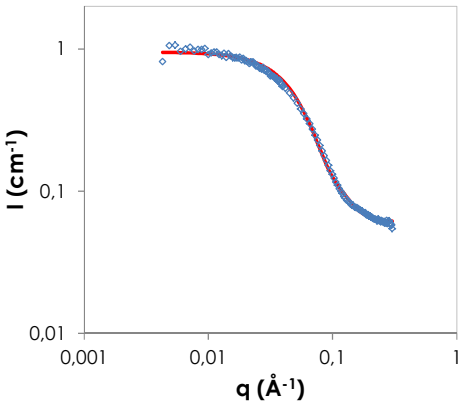

Figure S3: SANS pattern of BSA in PBS/D_2O at 13 mg/ml. The red line is a SANS model for ellipsoids obtained for R_a=1.35 nm, R_b= 4.8 nm dimension.

Guinier plots

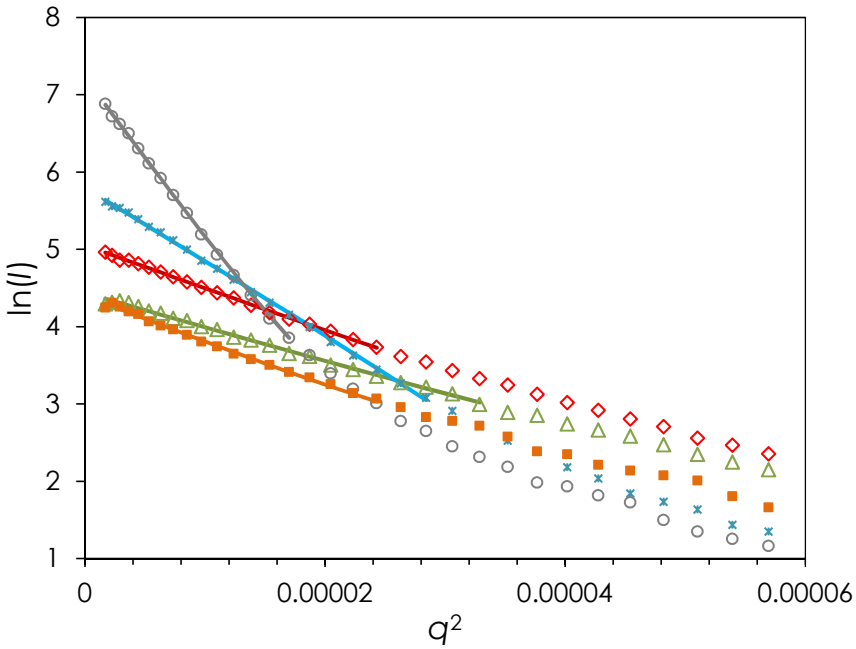

Figure S4: Guinier plots (ln(I) vs q^2) for the 0.4 mg/ml series. Red diamonds: SQAd in D2O; green triangles: SQAd with BSA; blue crosses: SQAd in PBS; grey circles SQAd in PBS after 2 hours; orange squares: SQAd in FBS/PBS. The continuous lines are the fits. The fitting values are obtained from SasView software.

SANS fits with lognormal distributions of spheres

In order to estimate the size distribution and volume fraction of SQAd nanoparticles in the samples, the SANS patterns of SQAd nanoparticles were fitted using SasView software[1] with the scattering length densities (SLD) reported in Table S1.

We used a lognormal distribution of spheres swollen by the solvent – as presented in our previous study.[1] For pure SQAd solutions, the fitting parameters are the following: nanoparticle radius (R), the polydispersity index (PD) and the swelling of the particles ($x_{solvent}$) as the volume fraction is known from composition.[1] For the mixtures of nanoparticles with BSA or FBS, the contribution of either BSA or FBS was subtracted beforehand. Then the fitting parameters are the nanoparticle radius (R), the polydispersity index (PD), and the volume fraction of the particles Φ_{SQAd} (assuming a constant swelling for the particles). As an example the fits of the SANS of SQAd nanoparticle in D_2O and in the presence of FBS are presented in Figure S5. The parameters used for all the SANS patterns presented in the manuscript are gathered in Table S2 and Table S3.

The decrease of the contribution of the SQAd nanoparticle scattering in the presence of BSA and FBS is estimated through the decrease of Φ_{SQAd}. Overall, we find the same orders of magnitude for

[1] The SasView application (www.sasview.org) was originally developed under NSF award DMR-0520547. SasView contains code developed with funding from the European Union's Horizon 2020 research and innovation programme under the SINE2020 project, grant agreement No 654000.

the loss percentage of nanoparticulate SQAd as with the use of linear combination of SANS patterns which are presented in the main manuscript.

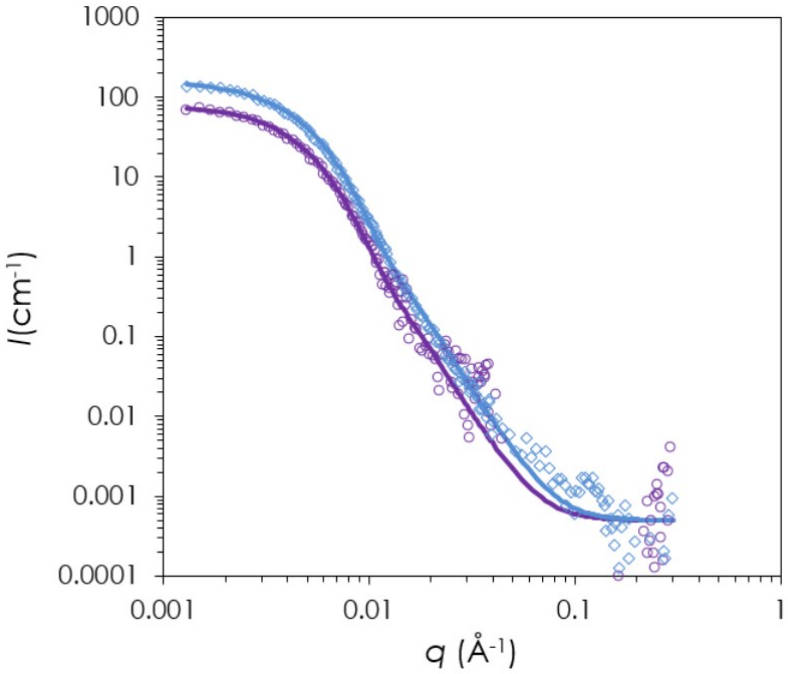

Figure S5: SANS pattern for SQAd nanoparticles in D_2O (blue diamonds) and corresponding fit with a lognormal distribution of spheres (blue line). Subtracted SANS pattern for SQAd nanoparticles in FBS ($I_{SQAD/FBS}$ - I_{FBS}, purple circles) and corresponding fit with a lognormal distribution of spheres (purple line)

Table S1: Scattering length densities (SLD) used for the fits. For the SQAd derivative the H/D exchange has been taken into account.

Component	SLD (10^{-10} cm^{-2})
SQAd	1.49
D_20	6.4

Table S2: Fitting parameters of SANS patterns obtained for 0.4 and 1 mg/ml SQAd in D_2O or in D_2O+BSA. Fit is obtained with a lognormal distribution of swollen SQAd spherical nanoparticles, Φ_{SQAd} is obtained from SQAd concentration for SQAd concentration for SQAd/D_2O and from fitting for SQAd/BSA mixtures, (R, PD) define the lognormal distribution in radius, $x_{solvent}$ is the volume fraction of solvent inside the particles, $\Phi_{SQAd,swell}$ is the total volume fraction of swollen nanoparticles in the solution and N the density number of particles in the solution.

Sample	[SQAd] mg/ml	Φ_{SQAd}	R (nm)	PD	$x_{solvent}$ in the NPs	$\Phi_{SQAd,swell}$	N part/cm^3
SQAd/D2O _bf	0.4	$4.0\ 10^{-4}$	30.2	0.3	0.57	$9.2\ 10^{-4}$	$5.7\ 10^{-12}$
SQAd/BSA/PBS	0.4	$3.1\ 10^{-4*}$	26.7	0.3	0.57	$7.2\ 10^{-4}$	$6.0\ 10^{-12}$
SQAd/D2O	1	$1.0\ 10^{-3}$	29.2	0.3	0.56	$2.3\ 10^{-3}$	$1.4\ 10^{-11}$
SQAd/BSA/PBS	1	$8.3\ 10^{-4**}$	28.5	0.3	0.56	$1.9\ 10^{-3}$	$1.3\ 10^{-11}$

*This corresponds to the loss of 22.5% SQAd nanoparticles.
**This corresponds to the loss of 16.5% SQAd nanoparticles.

Table S3: Fitting parameters of SANS patterns obtained for 0.4 and 1 mg/ml SQAD in D_2O or in D_2O+FBS. Fit is obtained with a lognormal distribution of swollen SQAd spherical nanoparticles, □$_{SQAd}$ is obtained from SQAd concentration for the SQAd/D_2O and from fitting for SQAd/FBS mixtures, (R, PD) define the lognormal

distribution in radius, $x_{solvent}$ is the volume fraction of solvent inside the particles, $\Phi_{SQAd,swell}$ is the total volume fraction of swollen nanoparticles in the solution and N the density number of particles in the solution.

Sample	[SQAd] mg/ml	Φ_{SQAd}	R (nm)	PD	$x_{solvent}$ in the NPs	$\Phi_{SQAd,swell}$	N part/cm^3
SQAd/D_2O	0.4	$4.0\ 10^{-4}$	30.2	0.3	0.57	$9.2\ 10^{-4}$	$5.7\ 10^{-12}$
SQAd/FBS/PBS	0.4	$2.0\ 10^{-4*}$	30.3	0.3	0.57	$4.7\ 10^{-4}$	$2.7\ 10^{-12}$

*This corresponds to the loss of 50% nanoparticulate SQAd.

SQAd nanoparticle disassembly with increasing BSA/SQAd ratio

Further SANS analysis in D_2O was performed at LLB, PAXY for a 0.5 mg/ml SQAd dispersion with increasing amount of BSA (6.5 to 13 mg/ml). In Figure S6, we repeatedly identify the decrease of the intensity in the low q range with increasing BSA concentration. The total volume fraction of SQAd nanoparticles is decreasing with increasing the amount of BSA in the solution.

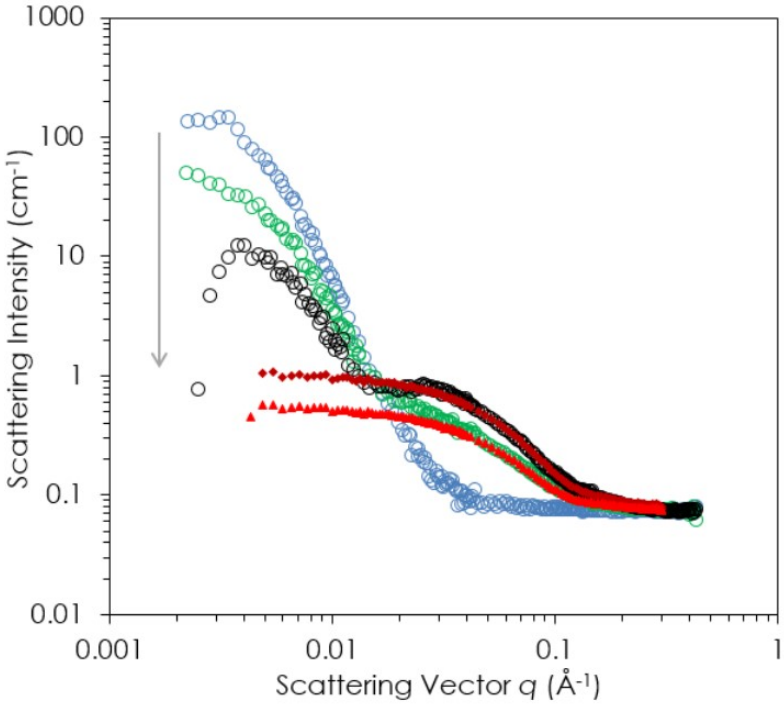

Figure S6: SANS patterns (LLB, PAXY) of SQAd nanoparticles with increasing BSA/SQAd ratios. **1)** 05 mg/ml SQAd in D_2O (blue circles) **2)** 0.5 mg/ml SQAd in the presence of BSA/D_2O at [BSA] = 6.5 mg/ml (green circles); i.e. a BSA/SqAd molar ratio of 0.147 (6.8 SqAd per BSA) **3)** 0.75 mg/ml SQAd in the presence of BSA/D_2O at [BSA] = 13 mg/ml (black circles); i.e. a SqAd/BSA molar ratio of 0.196 (5.1 SqAd per BSA).
SANS patterns of BSA at 6.5 (red triangles) and 13 mg/ml (red diamonds) in PBS are added for comparison.

For PAXY LLB experiments, four configurations were used to cover a q range going from 0.0022 to 0.42 Å^{-1} (wavelength: λ = 15 Å, sample to detector distance D = 6.7+0.035 m, standard two diaphragms geometry collimations: λ = 7.6, λ =12), (λ = 8.5 Å, D = 5+0.035, collimation Φ = 7.6, Φ = 12) (λ = 5 Å, D = 3.5+0.035 m, collimation λ =7.6, λ =16) (λ = 5 Å, D = 1.2+0.035 m, collimation Φ = 7.6, Φ = 22) for respectively very small angle, small angle, medium angle and large angle.

Repeatability of the salt-induced aggregation

The behavior of SQAd nanoparticles in PBS/D_2O for a 1 mg/ml SQAd solution is similar to the behavior described for a 0.4 mg/ml SQAd solution.

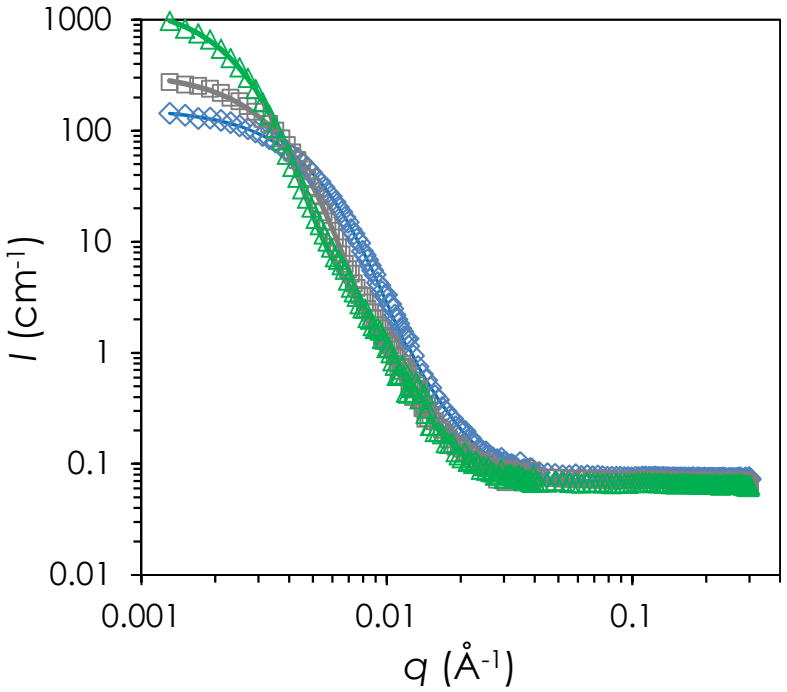

Figure S7: SANS patterns of SQAd nanoparticles (1 mg/ml) in 1) D_2O (blue diamonds), 2) PBS just after sample preparation (i.e. ~10 mn) (grey squares) and 3) PBS, >2h00 after sample preparation (green triangles). The colored lines are the corresponding fits with lognormal distributions of spheres.

Table 4: Evolution of the fitting parameters (with a lognormal distribution of spheres swollen by water) for SQAd suspension in D_2O or PBS

Sample	[SQAd] mg/ml	Φ_{SqAd}	*R* (nm)	PD	$x_{solvent}$ in the NPs	$\Phi_{SqAd,swell}$	N part/cm^3
SQAd/D2O	0.4	$4.0\ 10^{-4}$	30.2	0.3	0.57	$9.2\ 10^{-4}$	$5.8\ 10^{-12}$
SQAd/PBS *t*=10 min	0.4	$4.0\ 10^{-4}$	48.0	0.25	0.67	$1.2\ 10^{-3}$	$2.0\ 10^{-12}$
SQAd/PBS *t*=2h00	0.4	$4.0\ 10^{-4}$	72.0	0.25	0.57	$9.3\ 10^{-3}$	$3.9\ 10^{-13}$
SQAd/D2O	1	$1.0\ 10^{-3}$	29.2	0.3	0.56	$2.3\ 10^{-3}$	$1.4\ 10^{-11}$
SQAd/PBS *t*=10 min	1	$1.0\ 10^{-3}$	57.5	0.3	0.72	$3.5\ 10^{-3}$	$3.0\ 10^{-12}$
SQAd/PBS *t*=2h00	1	$1.0\ 10^{-3}$	99.1	0.3	0.75	$4.0\ 10^{-3}$	$6.9\ 10^{-13}$

3. Synchrotron radiation circular dichroism

Synchrotron radiation circular dichroism (SRCD) experiments were performed on the DISCO beamline at SOLEIL Synchrotron (Saint Aubin, France). 4 µL droplets of the samples were inserted in CaF_2 cells (Hellma) with a 3.7 µm path length. The raw spectra were acquired with a 1 nm spectral resolution. The spectra presented in this study were treated with the the CDTool software.[5] They are each the average

of three spectra. A background (water or corresponding buffer spectrum acquired in the same conditions) was subtracted from them. Intensity calibration was obtained with a camphor sulfonic acid CSA scale standard sample. Intensities were converted from millidegrees (θ machine units) into Δε using the formula $\Delta\varepsilon = \theta * \frac{0.1*MRW}{3298*l*C*3298}$, where MRW is the mean residue weight of the BSA (protein weight/number of residues = 114 Da), *l* is the path length of the CaF_2 cell in cm and *C* is the protein concentration in mg/ml. Occasionally we have added a smoothing function.

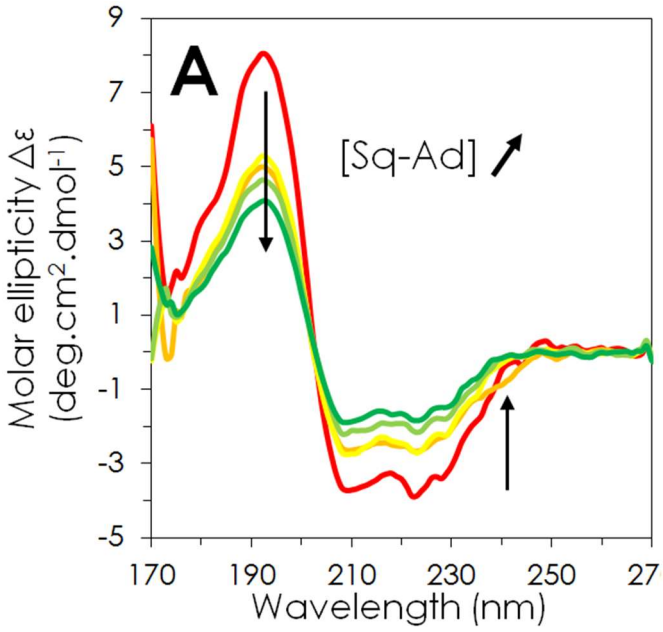

Figure S8: Dichroic spectra of BSA in presence of increasing concentrations of SQAd nanoparticles.

4. Fluorescence spectroscopy as a function of time

In order to assess the temporal evolution of the fluorescence emission of BSA-Sq-Ad NPs mixtures, the maximum of the fluorescence emission (348 nm) was monitored as a function of time during 16 hours, starting just after the mixing of the SQAd nanoparticles and BSA. The Figure S9 shows that fluorescence quenching of BSA occurs within a few seconds.

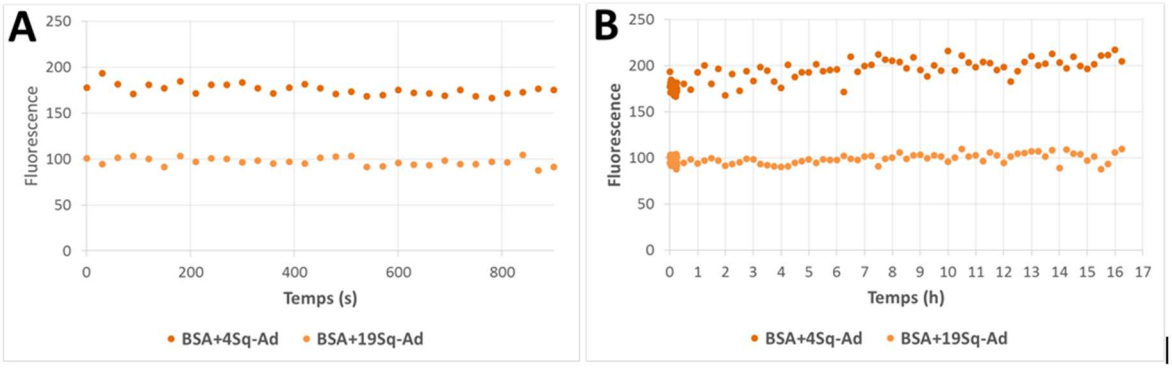

Figure S9: Fluorescence emission at 348 nm of two BSA:SQAd solutions (1 :4 and 1 :19 ratio) monitored as a function of time. **A)** During the 15 minutes following the mixing (Time resolution = 30 s) **B)** during the following 16 hours (time resolution = 15 min).

5. Isothermal Titration Calorimetry: dilution of SQAd nanoparticles

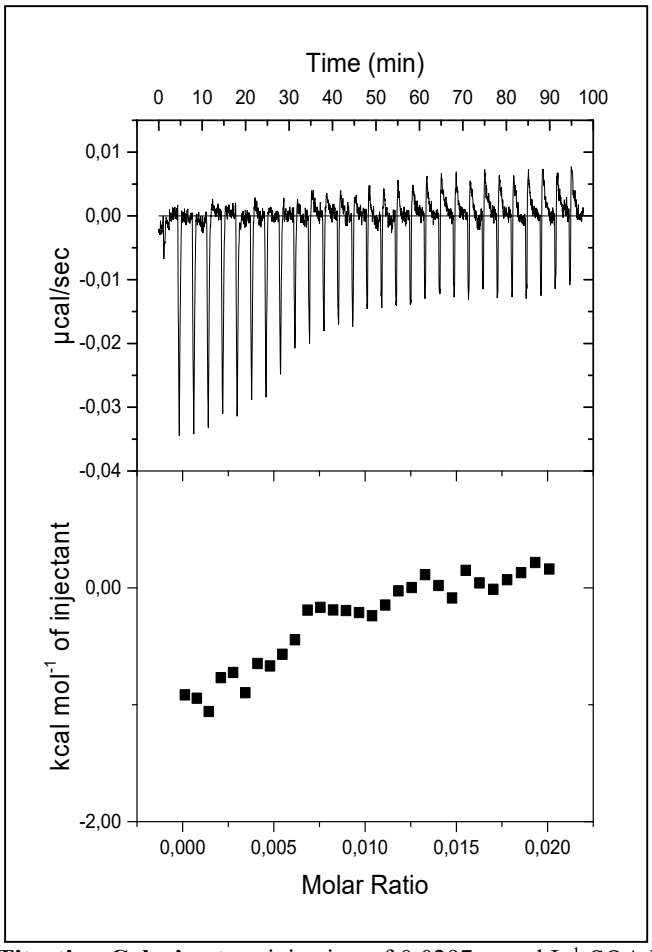

Figure S10: Isothermal Titration Calorimetry: injection of 0.0297 mmol.L^{-1} SQAd nanoparticles solution in pure water.

6. Interaction beween Squalene-Deoxycytidine (SQDc) nanoparticles and BSA probed by Fluorescence quenching and circular dichroism

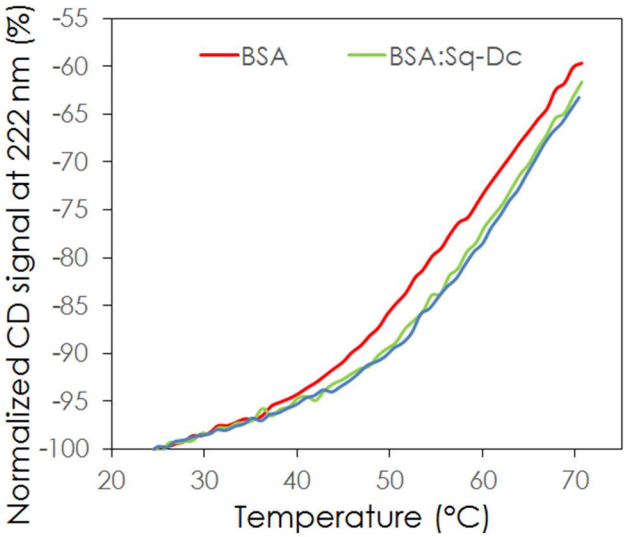

Figure S11: Thermal denaturation of BSA (red trace), BSA + SQDc nanoparticles (green trace) and BSA + SQAd nanoparticles (blue trace) with 11:1 molar ratio monitored with CD signal at 222 nm.

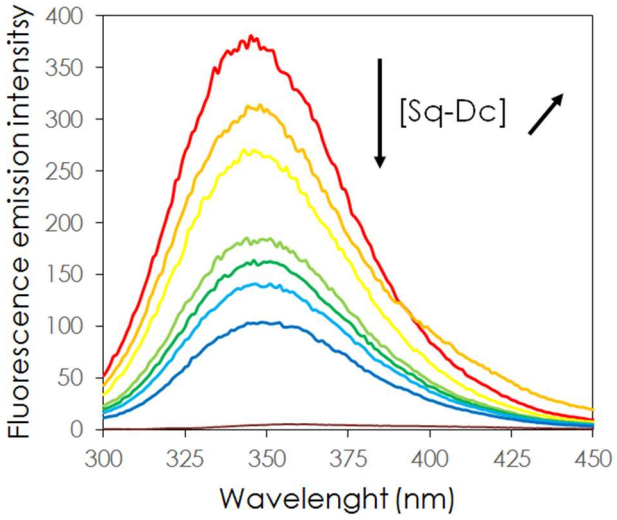

Figure S12: Characterization of BSA-SQDc interaction through fluorescence quenching experiments. A) Fluorescence emission spectra of BSA solutions quenched by an increasing concentration of SQDc nanoparticles. From red to blue: [SQDc]/[BSA] = 0, 1, 4, 9, 11, 14 and 19. The purple trace is the fluorescence emission of a SQDc solution without BSA.

7. Docking simulations

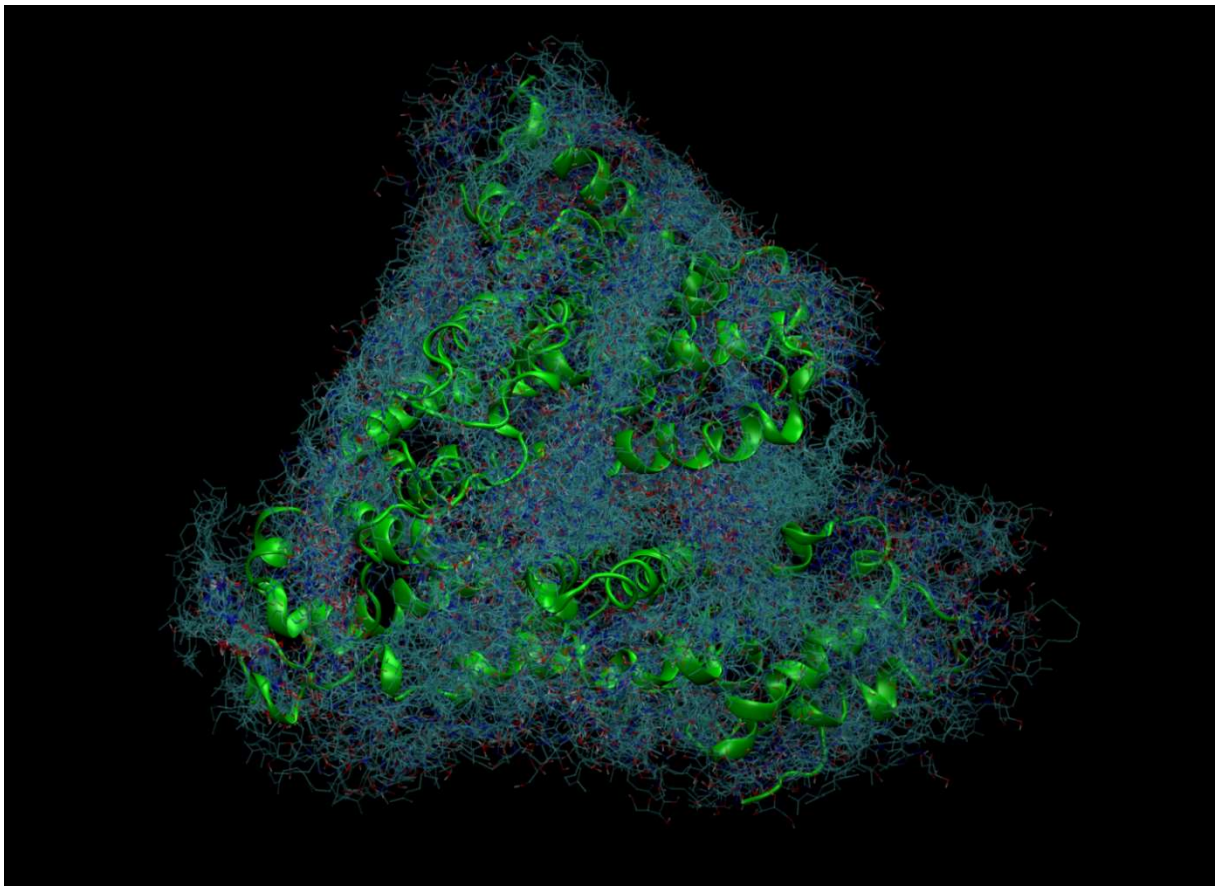

Figure S13: Best docking poses of SQAd for three randomly chosen protein frames. The protein is shown in green as cartoon representation while the ligands are shown in wireframe representation.

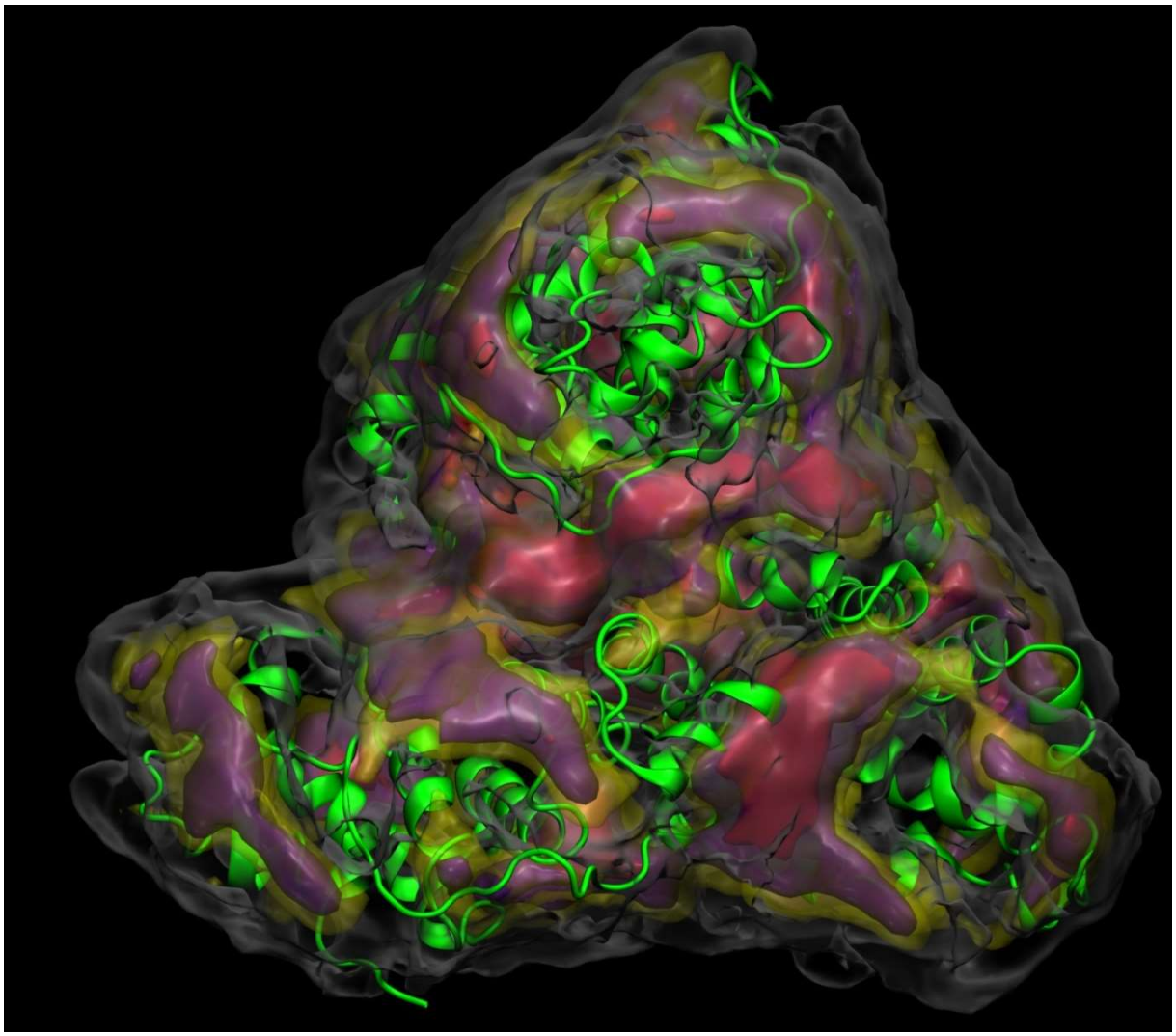

Figure 14: The density of ligand atoms around the protein. Three density isosurfaces are shown as semi-transparent shells. Red corresponds to the highest density, purple to intermediate density and white for low density. The protein is shown in green as cartoon representation.

Additional references

(1) Saha, D.; Testard, F.; Grillo, I.; Zouhiri, F.; Desmaele, D.; Radulescu, A.; Desert, S.; Brulet, A.; Couvreur, P.; Spalla, O. The Role of Solvent Swelling in the Self-Assembly of Squalene Based Nanomedicines. *Soft Matter* **2015**, *11* (21), 4173–4179. https://doi.org/10.1039/C5SM00592B.

(2) Bendedouch, D.; Chen, S. H. Structure and Interparticle Interactions of Bovine Serum Albumin in Solution Studied by Small-Angle Neutron Scattering. *J. Phys. Chem.* **1983**, *87* (9), 1473–1477. https://doi.org/10.1021/j100232a003.

(3) Nossal, R.; Glinka, C. J.; Chen, S.-H. SANS Studies of Concentrated Protein Solutions. I. Bovine Serum Albumin. *Biopolymers* **1986**, *25* (6), 1157–1175. https://doi.org/10.1002/bip.360250613.

(4) Zhang, F.; Skoda, M. W. A.; Jacobs, R. M. J.; Martin, R. A.; Martin, C. M.; Schreiber, F. Protein Interactions Studied by SAXS: Effect of Ionic Strength and Protein Concentration for BSA in Aqueous Solutions. *J. Phys. Chem. B* **2007**, *111* (1), 251–259. https://doi.org/10.1021/jp0649955.

(5) Lees, J. G.; Smith, B. R.; Wien, F.; Miles, A. J.; Wallace, B. A. CDtool—an Integrated Software Package for Circular Dichroism Spectroscopic Data Processing, Analysis, and Archiving. *Analytical Biochemistry* **2004**, *332* (2), 285–289. https://doi.org/10.1016/j.ab.2004.06.002.